Nanoscale

ROYAL SOCIETY OF CHEMISTRY

PAPER

View Article Online
View Journal | View Issue

Check for updates

Cite this: *Nanoscale*, 2022, **14**, 1296

One-step fabrication of eco-friendly superhydrophobic fabrics for high-efficiency oil/water separation and oil spill cleanup†

Haiyang Yu,‡[a] Min Wu, ‡[b] Gaigai Duan [c] and Xiao Gong *[a]

The oily wastewater and oil spill caused by oil leakage accidents are extremely harmful to human health and the environment. Thus, it is very important to exploit superhydrophobic separation materials and technologies for oil/water separation and oil spill cleanup. In this study, using the 1,4-conjugate addition reaction between polyethyleneimine (PEI) and 3-(trimethoxysilyl)propyl acrylate (TMSPA), hydrolysis condensation reaction of TMSPA and dodecyltrimethoxysilane (DTMS) jointly connecting to the surface of hydrophilic silica nanoparticles, and hydrogen bond interaction of the residual amino group on the surface of PEI, covalently-crosslinked rough network structures were constructed on fabric surfaces, which endow PEI/TMSPA/SiO_2/DTMS fabrics with excellent superhydrophobic properties. The obtained superhydrophobic fabric not only showed excellent heat resistance and excellent stability to acid, alkali, salt and organic solvents, but also showed good mechanical stability to tape stripping and washing tests. The superhydrophobic, superoleophilic properties and porous structure of the modified fabric make it have excellent oil/water separation efficiency (98.49% after 18 cycles) and oil spill cleanup efficiency (95.35% after 9 cycles). This superhydrophobic PEI/TMSPA/SiO_2/DTMS fabric has characteristics of simple preparation, environmental friendliness and scale-up, which makes it a very promising separation material for actual oil/water separation and oil spill cleanup.

Received 27th October 2021,
Accepted 22nd December 2021

DOI: 10.1039/d1nr07111d

rsc.li/nanoscale

Published on 22 December 2021. Downloaded on 1/19/2026 7:56:09 PM.

1. Introduction

Spilled oil in oceans caused by oil leakage accidents not only brings severe challenges to the oil spill cleanup but also seriously pollute the marine environment and damage the marine ecology. In addition, due to the toxic chemical substances in industrial oily wastewater, arbitrary discharging of it is extremely harmful to human health and the environment. Thus, it is urgent to exploit effective materials or technologies for the separation and collection of oil and organic pollutants in wastewater. In particular, oil-absorbing materials with low cost and high absorbability have attracted much attention. At present, a variety of treatment methods have been developed, such as water purification technology,[1,2] membrane technology,[3–5] and oil-absorbing materials[6] for oil-spill cleanup on seas. However, developing oil absorbent materials with high separation efficiency, high reusability and excellent recyclability remain a huge challenge.

Superhydrophobic materials with water contact angle (WCA) >150° have shown great potentials in anti-ice,[7,8] drag reduction,[9,10] self-cleaning,[11,12] droplet manipulation,[13,14] oil/water separation[15–18] and so on. Inspired by natural lotus leaves, rose petals, gecko, and water striders, researchers have prepared superhydrophobic surfaces using a strategy of constructing graded rough structures with micro/nanomaterials and modifying surfaces with low surface energy substances.[19] Among numerous superhydrophobic materials, waterproof textiles are considered to be the ideal choice for the treatment of oily wastewater or cleanup of the oil spill in oceans. Textile like cotton fabric is cheap, widely available, flexible and elastic, showing a potential application value.[20] However, the pristine fabric absorbs both oil and water. The functional modification gives the superhydrophobic and superoleophilic fabric the capability to effectively absorb oil and completely

[a]*State Key Laboratory of Silicate Materials for Architectures, Wuhan University of Technology, Wuhan 430070, P. R. China. E-mail: xgong@whut.edu.cn*
[b]*Huaxi MR Research Center (HMRRC), Department of Radiology, Functional and Molecular Imaging Key Laboratory of Sichuan Province, West China Hospital, Sichuan University, Chengdu, 610041, China*
[c]*Jiangsu Co-Innovation Center of Efficient Processing and Utilization of Forest Resources, International Innovation Center for Forest Chemicals and Materials, College of Materials Science and Engineering, Nanjing Forestry University, Nanjing, 210037, China*

†Electronic supplementary information (ESI) available. See DOI: 10.1039/d1nr07111d

‡Equal contribution.

This journal is © The Royal Society of Chemistry 2022

Published on 22 December 2021. Downloaded on 1/19/2026 7:56:09 PM.

repel water, achieving oil/water mixture separation and oil spill cleanup.

In recent years, a variety of techniques such as dip-coating,[21] hydrothermal method,[22] atomic layer deposition,[23] chemical vapor deposition[24] and plasma etching process[25] have been introduced to produce superhydrophobic coatings on fabrics. However, some of these preparation methods are either time-consuming or have complicated manufacturing processes, while others have disadvantages of complex equipment and the inability to prepare on a large scale. Fluorinated chemicals like fluorosilane are widely used in preparing superhydrophobic coatings due to extremely low surface energy, but they are extremely harmful to human health and the environment. Therefore, in order to overcome the above shortcomings, it is still challenging to develop one-step, environmentally friendly, large-scale strategies to fabricate superhydrophobic/superoleophilic fabrics for oil–water separation and oil absorption. In addition, superhydrophobic fabrics with good stability and high durability as well as excellent reusability deserve further research.

Polyethyleneimine (PEI) is a water-soluble branched polymer. Due to its rich amino and hyperbranched structures, PEI provides a unique opportunity to construct advanced PEI derivatives and prepare functional materials.[26] Manna *et al.*[27–30] used a simple and robust 1,4-conjugate addition reaction between the primary amine group of branched polyethyleneimine (BPEI) and the acrylate group of dipentaerythritol penta-acrylate (5Acl), and then made an appropriate post-chemical modification to prepare a series of functional super-wetting materials. However, both the self-assembly method and post-modification process are inevitable to the problems of cumbersome preparation. Sohail *et al.*[31] reported poly(propylene) (PP) films could be surface modified with 3-(trimethoxysilyl)propyl acrylate (TMSPA) by the silanization reaction, causing it suitable for covalently bonding with UV-curable coatings.

In this work, based on the post-functionalization properties of the PEI/acrylate group modifying coating, we designed a novel surface functional strategy to realize the multi-functional covalent cross-linking of PEI and TMSPA through 1,4-conjugate addition reaction and used DTMS and hydrophilic silica nanoparticles to modify the surface of cotton fabrics, so as to produce durable superhydrophobic cotton fabrics. This is the first report on the fabrication of super-wetting materials by PEI/TMSPA coating. The whole process was completed in one step without using fluorinated chemicals, which is simple, environmentally friendly and easy to prepare on a large scale. Due to its superhydrophobicity and superoleophilicity, the modified cotton fabric has high oil flux and excellent oil–water separation efficiency (98.49% after 18 cycles). At the same time, the coated fabric was further made into a mini boat to effectively collect oil, showing excellent oil spill cleanup efficiency (95.35% after 9 cycles). In addition, the modified cotton fabric shows excellent heat resistance, chemical stability, reusability and good mechanical durability.

2. Experimental section

Materials

Polyethyleneimine (PEI; M_n = 60 000) was purchased from Sigma-Aldrich. 3-(Trimethoxysilyl)propyl acrylate (TMSPA) and dodecyltrimethoxysilane (DTMS) were purchased from Aladdin Industrial Co., Ltd. Hydrophilic gas-phase nano-silica (7–40 nm) and Sudan IV were bought from Macklin Biochemical Co., Ltd (Shanghai). Cotton fabric, silk, polyester, ramie and acrylic fabric were purchased from local stores.

Preparation of superhydrophobic cotton fabric

Superhydrophobic PEI/TMSPA/SiO_2/DTMS cotton fabric was fabricated using a one-step approach. The typical preparation process is as follows: cotton fabrics were cleaned in acetone and ethanol by ultrasonication for 10 min and dried for later use. Certain amounts of TMSPA and DTMS were dispersed in 20 mL ethanol solution, and 20 mL PEI aqueous solution (10 mg mL^{-1}) was dropped into the mixture solution with stirring. The final concentration of TMSPA was 0–4 μL mL^{-1}, and the concentration of DTMS was 10 μL mL^{-1}. Then, hydrophilic silica nanoparticles (0–10 mg mL^{-1}) were placed in the above solution, which was ultrasonically treated for 5 min. Finally, the fabrics were placed in the mixed solution, which was magnetically stirred at 500 rpm for 4–20 h at 25 °C. The cotton fabric was washed with water and ethanol. Then, it was dried at 80 °C for 2 h. PEI and TMSPA co-modified silica nanoparticles were prepared by the same steps as above, merely without DTMS and the cotton fabric.

Characterizations

The morphology of the coated cotton fabric was examined using field emission scanning electron microscopy (FE-SEM, Zeiss Ultra Plus, Germany). An energy dispersive spectrometer (EDS, Hitachi S-4800) combined with SEM was used to determine the element distribution of the samples. We used Fourier transform infrared spectrometer (FTIR, Nicolet 6700, Thermoelectric Scientific Instruments Corp, USA) to detect the chemical composition of PEI and TMSPA co-modified silica. The chemical composition of the original and superhydrophobic fabrics was detected using the attenuated total reflectance Fourier transform infrared spectrometer (ATR-FTIR, Nicolet 6700, Thermoelectric Scientific Instruments Corp, USA). The elemental composition of the fabrics was systematically characterized using X-ray photoelectron spectroscopy (XPS, AXIS SUPRA). A droplet shape analyzer (DSA100, Kruss, Germany) was used to measure water contact angles (WCAs) using 2 μL deionized water. In order to reduce the measurement error, WCA was measured in five different positions for each sample, and the average value was then calculated. The organic carbon content in water was assessed using a Total organic carbon analyzer (TOC-L-CPN, Shimadzu, Japan) and the oil content was obtained by conversion.

Stability evaluation

The heat resistance of PEI/TMSPA/SiO_2/DTMS fabrics was tested by measuring the WCA after heating for 2 h at the inter-

Published on 22 December 2021. Downloaded on 1/19/2026 7:56:09 PM.

val of 20 °C at 100–180 °C. PEI/TMSPA/SiO_2/DTMS fabrics were irradiated at a distance of 15 cm using a ultraviolet lamp (1000 W) for 2 min per cycle to evaluate their UV resistance. To evaluate the chemical stability, PEI/TMSPA/SiO_2/DTMS fabrics were immersed in 1 M NaCl, NaOH, and HCl solution for 12 h, respectively. WCAs were recorded every 2 h. PEI/TMSPA/SiO_2/DTMS fabrics were put in a variety of organic solvents such as dichloromethane, *n*-hexane, ethyl acetate, DMF, ethylene glycol, toluene and acetone, which has different polar parameters. The cotton fabric sample was washed and dried after impregnation, and its WCA was then measured. The mechanical stability of PEI/TMSPA/SiO_2/DTMS fabrics was analyzed by peeling test and washing test. For the adhesive tape peeling test, we used adhesive tape pressure on the PEI/TMSPA/SiO_2/DTMS fabric and then tore it. The adhesive tape was replaced by a new one every 10 peeling tests to maintain strong adhesion. The washability of PEI/TMSPA/SiO_2/DTMS fabrics was measured on the basis an improved standard method (ISO 105-C10:2006 (C)).[32] In short, the fabrics were washed by stirring in aqueous solutions with a 0.5 wt% detergent at 40 °C and 150 rpm. Each washing cycle lasted 30 minutes.

Oil/water separation and oil spill cleanup

Oil and water in equal volumes were mixed to prepare the oil/water mixture. The coated fabric was placed between two glass containers as a separation layer to separate the oil/water mixtures. The separation could be completely achieved by gravity. The water mass before and after separation, oil mass after separation and separation time of the oil/water mixtures were recorded. To study the recoverability of the coated fabrics, the oil/water separation process was repeated for 18 cycles. The superhydrophobic fabrics were washed with ethanol and then dried for later use after each separation process. Flux and separation efficiency were calculated using the following equations:

$$\text{Flux} = \frac{V}{\text{St}} \tag{1}$$

$$E_{\text{ff}} = \left(\frac{M_{\text{b}}}{M_{\text{a}}}\right) \times 100\% \tag{2}$$

where V (L) is oil permeation volume, S (m^2) is the contact area, and t (h) is the recorded oil permeation time. M_a and M_b are water mass before and after separation.

The superhydrophobic mini boat was made of copper mesh as the skeleton and coated with superhydrophobic fabric for oil spill cleanup. In the oil spill cleanup test, a certain amount of octane was poured into a water-rich beaker to simulate the oil spill. The fabricated superhydrophobic mini boat was then put in the beaker to make oil spill cleanup with self-driving. After each cleanup process, the boat was cleaned in ethanol and then dried for later use. The rate of cleanup can be calculated using the eqn (3):

$$\text{CR} = \frac{W_{\text{a}} + W_{\text{b}}}{W_{\text{o}}} \times 100\% \tag{3}$$

where CR is oil spill cleanup rate, W_o, W_a and W_b are weights of the original spilled oil, absorbed oil, and collected oil by the boat, respectively.

The oil-in-water emulsion was made using water and oil with a volume ratio of 49 : 1, in which Tween 80 was used as a surfactant. In the typical preparation process, water (49 mL), toluene (1 mL) and Tween 80 (40 mg) were mixed and ultrasonically treated for 15 min to finally form a stable emulsion solution. The separation efficiency (E_{ff}) was calculated using the following eqn (4):

$$E_{\text{ff}} = \left(1 - \frac{C}{C_0}\right) \times 100\% \tag{4}$$

where C_0 and C are the concentrations of oil in the original emulsion and the treated filtrate, respectively.

3. Results and discussion

Preparation of superhydrophobic PEI/TMSPA/SiO_2/DTMS fabrics

Scheme 1 shows the preparation process of superhydrophobic PEI/TMSPA/SiO_2/DTMS fabrics. First, the PEI aqueous solution was mixed with TMSPA and DTMS ethanol solution to form a mixed solution, and the 1,4-conjugate addition reaction occurred between PEI and TMSPA. Then, hydrophilic nanosilica particles were ultrasonically dispersed in the above mixtures, and hydrolysis and condensation of TMSPA and DTMS were co-modified on the surface of silica nanoparticles. Simultaneously, the clean fabric was immersed in the mixed solution. PEI could be adsorbed and fixed on the fiber surface, therefore, the covalently-crosslinked rough network structure was constructed on the fabric surface. The covalently-crosslinked network could fix the rough structure and reduce the surface energy because of many hydrophobic alkyl chains possessed by DTMS, which makes the obtained cotton fabric have excellent superhydrophobicity.

Surface morphologies and chemical compositions of superhydrophobic PEI/TMSPA/SiO_2/DTMS fabrics

Fig. 1a–d shows morphologies of the pristine and PEI/TMSPA/SiO_2/DTMS fabrics. The fiber surface of the original fabric shows a smooth surface. Because the original fabric surface has abundant hydroxyl groups, it shows superhydrophilicity with a WCA of ~0°. After a simple one-step deposition PEI/TMSPA/SiO_2/DTMS coating of 7.5 mg mL^{-1} SiO_2, many microparticles (Fig. 1c) and a small amount of nano-sized particles (Fig. 1d) were observed on the coated fabric surface. The WCA of the coated fabric was 155.0 ± 0.8°, showing excellent superhydrophobicity. Besides, the morphology of the fabric surface modified by SiO_2 nanoparticles with various concentrations (0, 2.5, 5, 10 mg mL^{-1}) is shown in Fig. S1.† It can be seen that SiO_2 nanoparticle concentration plays an important role in regulating the morphology of the coated fabrics. The surface of PEI/TMSPA/DTMS fabric is relatively smooth, with only a small number of protrusions caused by the polymer. After introdu-

 This journal is © The Royal Society of Chemistry 2022

Published on 22 December 2021. Downloaded on 1/19/2026 7:56:09 PM.

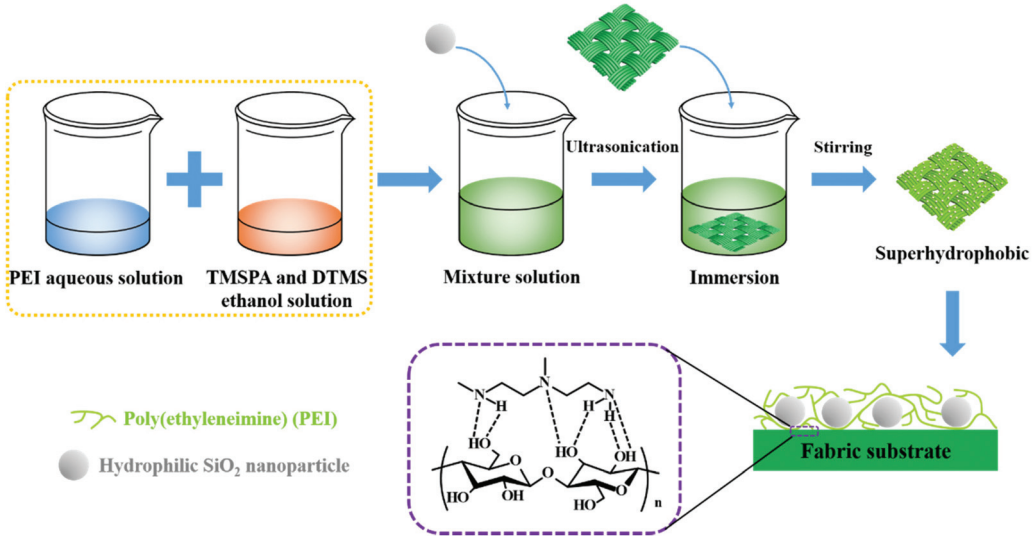

Scheme 1 Schematic of fabrication of superhydrophobic PEI/TMSPA/SiO_2/DTMS fabrics.

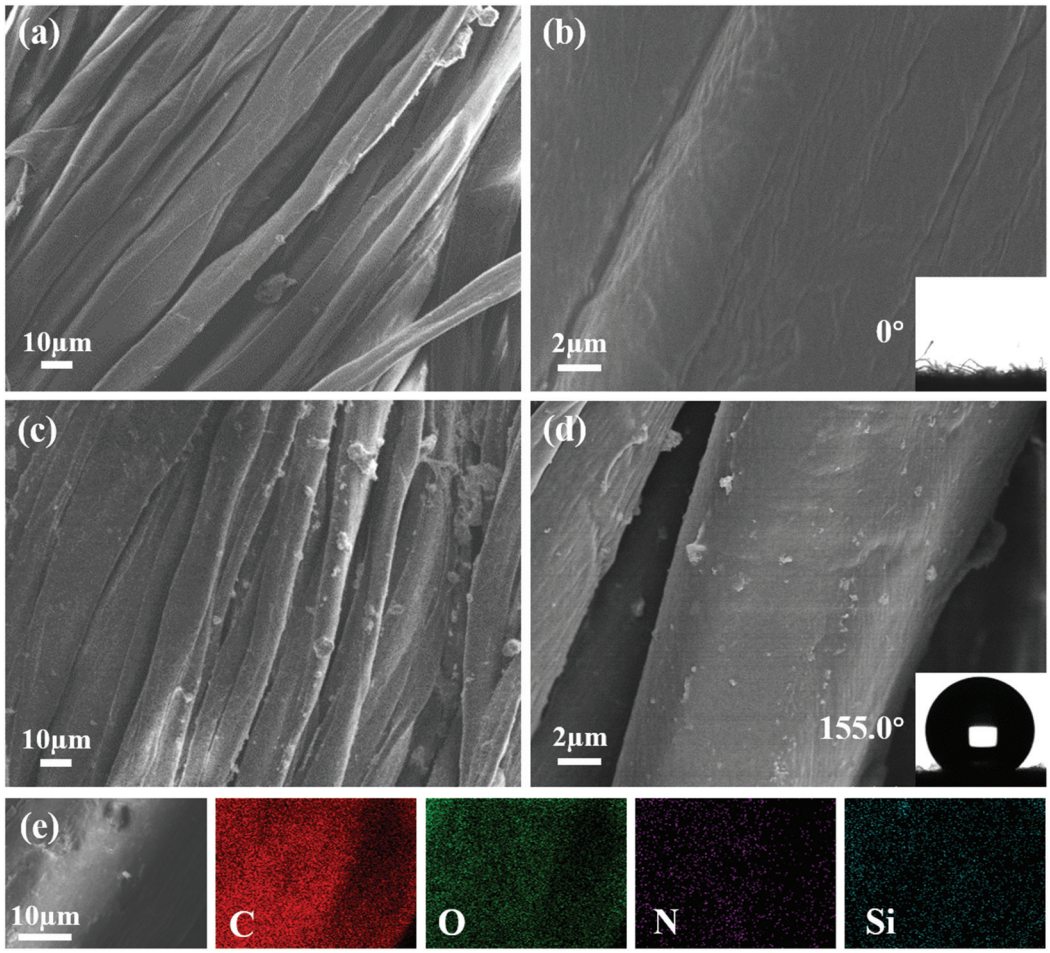

Fig. 1 SEM photographs of (a and b) the pristine fabric and (c and d) the PEI/TMSPA/SiO_2/DTMS fabric with 7.5 mg mL^{-1} SiO_2 nanoparticles. The insets in (b) and (d) are corresponding WCAs. (e) SEM-EDS mapping image of the coated fabric.

Published on 22 December 2021. Downloaded on 1/19/2026 7:56:09 PM.

cing SiO_2 nanoparticles, more micron-scale rough structures were detected when the concentration was increased. When the concentration of SiO_2 nanoparticles was increased to 7.5 mg mL^{-1}, the coated fabric achieved the best superhydrophobic performance, which is attributed to abundant air intercepted in the rough structures, largely improving the superhydrophobic properties of the coated fabrics. When the content of SiO_2 was increased to 10 mg mL^{-1}, a large number of nanosized particles were agglomerated due to the supersaturated micron-scale rough structure on the coated fabric fiber surface, thus the superhydrophobicity of the coated fabric was limited and WCA decreased slightly. EDS attached to the SEM was used to detect the chemical composition of the coated fabrics. The SEM-EDS mapping image and EDS spectrum showed that C, O, N and Si elements were evenly distributed on the fabric surface (Fig. 1e and S2†), indicating the uniform coverage of the PEI/TMSPA/SiO_2/DTMS coating on the fabric.

FTIR spectra confirmed the 1,4-conjugate addition reaction and chemical composition of the modified SiO_2 surface, and the successful modification of modified-SiO_2 on the superhydrophobic cotton fabric surface (Fig. 2). In the spectrum of TMSPA, the absorption peaks of –C═O stretching vibration from –COO–, symmetric deformation of C–H bond for the β carbon of the vinyl group, and –Si–O–Si– stretching vibrations are obviously seen at 1726 cm^{-1}, 1409 cm^{-1}, and 1088 cm^{-1}, respectively (Fig. 2a).[27] Characteristic peaks of TMSPA at 2946 cm^{-1} and 2842 cm^{-1} correspond to stretching vibrations of $–CH_3$ and $–CH_2–$. The PEI-TMSPA-SiO_2 spectrum exhibits a strong characteristic peak of –Si–O–Si– structure at 1097 cm^{-1}, as verified by the spectrum of pure SiO_2. Compared with the spectrum of pure SiO_2, the spectrum of PEI-TMSPA-SiO_2 exhibits extra characteristic peaks at 2957 cm^{-1} (inset in Fig. 2a) and 1728 cm^{-1}, corresponding to $–CH_2–$ stretching vibration of PEI or TMSPA derivative and –C═O stretching vibration of –COO– in TMSPA, respectively, as confirmed from the spectrum of pure PEI and TMSPA. These results showed that PEI and TMSPA were grafted onto the SiO_2 particle surfaces successfully. Furthermore, compared with the spectrum of pure TMSPA, the characteristic peak of the C–H bond for the β carbon of the vinyl group in the spectrum of PEI-TMSPA-SiO_2 disappeared at 1409 cm^{-1}, indicating that the 1,4-conjugate addition reaction between PEI and TMSPA successfully consumed the C═C bond.

FTIR spectra of original, PEI/SiO_2/DTMS, and PEI/TMSPA/SiO_2/DTMS fabrics are shown in Fig. 2b. Compared with the pristine fabric, the characteristic peaks at 2919 cm^{-1} and 2851 cm^{-1} in PEI/SiO_2/DTMS fabric were significantly enhanced, which corresponded to the symmetric and asymmetric stretching vibrations of $–CH_2–$ from DTMS,[33,34] revealing that DTMS was modified on the surfaces of the fabrics. The new absorption peaks at 1541–1578 cm^{-1} are ascribed to the bending vibration of the N–H bond, indicating that PEI has been successfully introduced on the surfaces of the fabric.[35] In the spectrum of the PEI/TMSPA/SiO_2/DTMS fabric, symmetric stretching vibration and asymmetric stretching vibration peak intensities of $–CH_2–$ decreased significantly, indicating that the grafting amount of DTMS on the fabric surface was reduced. The possible reason is that there is a competition between TMSPA and DTMS, and they all need to connect to the hydrophilic silica surface through the hydrolysis condensation reaction of silane groups.

XPS was also used to measure the chemical structure of the pristine and PEI/TMSPA/SiO_2/DTMS fabrics. As shown in Fig. 3a, the surface of the pristine fabric exhibits C 1s and O 1s peaks, but PEI/TMSPA/SiO_2/DTMS fabric surface shows three new peaks, namely, N 1s (399.00 eV), Si 2s (153.97 eV) and Si 2p (102.90 eV), corresponding to the characteristics covalent bonds N and Si. Fig. 3b presents the high-resolution C 1s spectrum of the pristine fabric, which can be deconvoluted into three peaks designated as the C–C/C–H bond at 284.72 eV, the C–N/C–O bond at 286.27 eV, and the C═O bond at 287.72 eV, respectively. As shown in Fig. 3c, the binding energies of the C–C/C–H bond, C–N/C–O bond and C═O bond in the high-resolution C 1s spectra of the PEI/TMSPA/SiO_2/DTMS fabric are 284.74 eV, 286.42 eV, and 288.09 eV, respectively.[36,37] The increase in the ratio of $–CH_x$ (C–C and C–H) is ascribed to the long alkyl chain in DTMS. Fig. 3d shows the high-resolution Si 2p spectrum of PEI/TMSPA/SiO_2/DTMS fabric with two peaks of 102.48 eV and 103.20 eV after deconvolution, attributed to the Si–C bond and Si–O bond. The Si content was 16.9 wt% for the PEI/TMSPA/SiO_2/DTMS fabric. Furthermore, the high-resolution N 1s spectrum (Fig. 3e) showed three different binding energies of N 1s at 398.85 eV, 399.45 eV and 401.19 eV, attributed to –N═, –NH–, and $–NH_2$/protonated nitrogen (N^+),[38,39] indicating that PEI molecules are connected to TMSPA and fabric surface by covalent bond and weak interaction forces, respectively. The above results showed that DTMS and PEI existed in the modified fabric, which is in agreement with FTIR analysis results. It is noteworthy that the atomic concentrations of –NH– and $–NH_2$/protonated nitrogen (N^+) are 48.21% and 22.0%, respectively. The contents of primary amine, secondary amine, and tertiary amine in PEI are 25%, 41%, and 34%, respectively, as reported.[40] The relative increase in the –NH– content and the relative decrease in the $–NH_2$/protonated nitrogen (N^+) content may indicate that the primary amine group forms secondary amine through the 1,4-conjugate addition reaction.

The proposed mechanism of the fabrication process

Based on the results of FTIR and XPS analyses, a mechanism for the formation of a covalently cross-linked rough network structure on the fabric surface is proposed (Fig. 4). TMSPA and DTMS can be jointly connected to the surface of hydrophilic silica nanoparticles *via* a hydrolysis condensation reaction. At the same time, the primary amino group of PEI and the acrylate group on the surface of silica nanoparticles is covalently connected by 1,4-conjugate addition reaction,[27] forming a covalently cross-linked network structure. In addition, the residual amino group on the PEI surface provides sufficient adhesion for fixing particles onto the fabric surfaces through interactions between hydrogen bonds,[41] so as to construct a stable rough structure. Finally, silica nanoparticles with low

 This journal is © The Royal Society of Chemistry 2022

Published on 22 December 2021. Downloaded on 1/19/2026 7:56:09 PM.

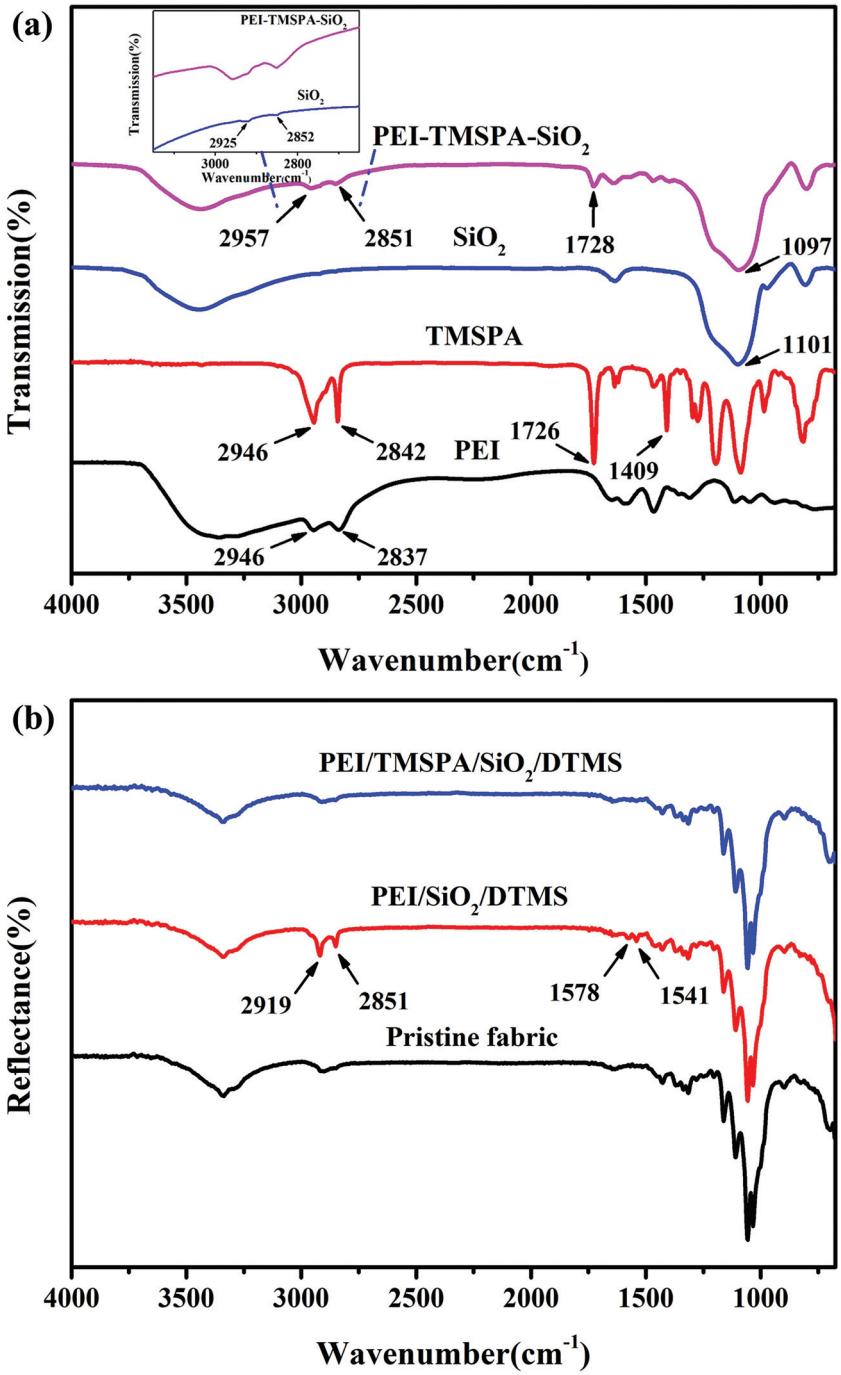

Fig. 2 FTIR spectra of (a) PEI-TMSPA-SiO_2, pure SiO_2, TMSPA and PEI, and (b) pristine fabric, PEI/SiO_2/DTMS fabric and PEI/TMSPA/SiO_2/DTMS fabric.

surface energy alkyl chains endow cotton fabric with superhydrophobicity.

Wettability and self-cleaning properties of superhydrophobic PEI/TMSPA/SiO_2/DTMS fabrics

The experimental design was optimized to obtain the best superhydrophobic performance, and the effect of reaction time, SiO_2 concentration and TMSPA concentration on the wettability of the PEI/TMSPA/SiO_2/DTMS fabric was studied. As shown in Fig. S3a,† the hydrophobicity first increased and then deteriorated with the reaction time increasing. The optimal performance was obtained once the reaction time was 12 h. With the increase of SiO_2 concentration, the WCA increased first, and then slightly decreased (Fig. S3b†). Similarly, when TMSPA concentration increased, the WCA increased and then decreased too (Fig. S3c†). The possible

Published on 22 December 2021. Downloaded on 1/19/2026 7:56:09 PM.

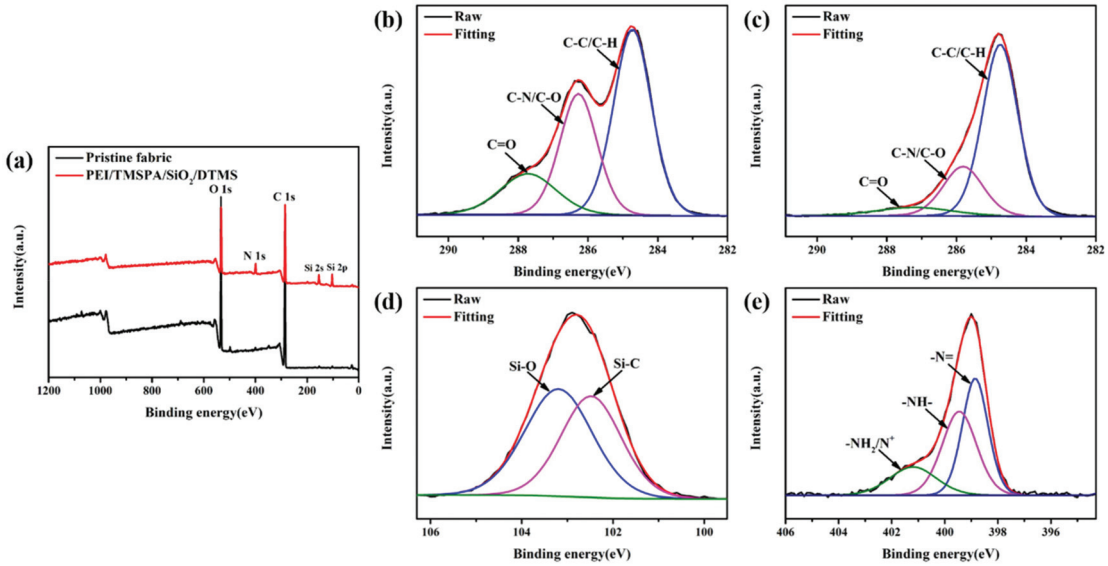

Fig. 3 (a) XPS spectra of pristine and PEI/TMSPA/SiO_2/DTMS fabrics. C 1s XPS spectra with fitting curves of (b) pristine and (c) PEI/TMSPA/SiO_2/DTMS fabrics. (d) Si 2p XPS spectra and (e) N 1s XPS spectra with fitting curves of the PEI/TMSPA/SiO_2/DTMS fabric.

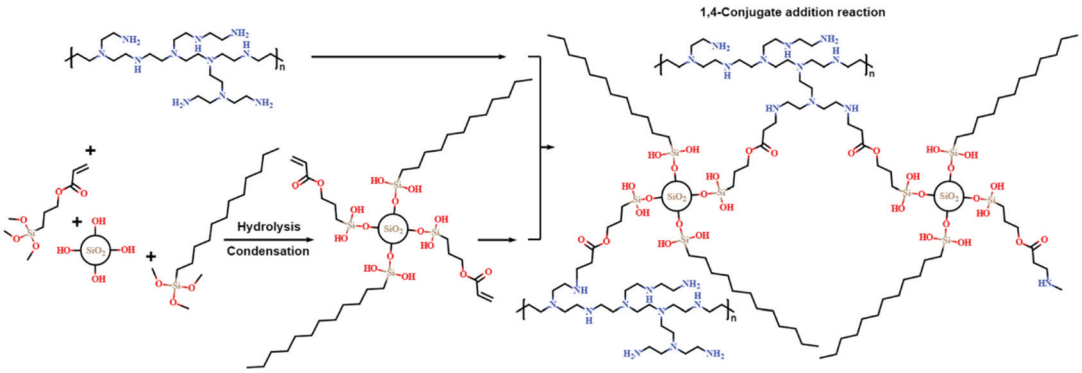

Fig. 4 Schematic illustration of a mechanism of superhydrophobic fabric during the fabrication process.

reason is that the covalently cross-linked network formed by TMSPA participating in 1,4-conjugate addition reaction can fix more nanoparticles with the increase in concentration. However, TMSPA has a competitive relationship with DTMS, further increase in concentration reduces the grafting amount of DTMS and leads to the decrease in hydrophobicity. Based on the above results, the surface wettability of the fabric modified with 12 h reaction time, 7.5 mg mL^{-1} SiO_2 and 2 μL mL^{-1} TMSPA was further studied.

Fig. 5a shows pictures of aqueous droplets on the pristine and coated fabric surfaces. Due to the porosity of the fabric and the capillary effect resulting from a lot of hydrophilic hydroxyl groups, pristine cotton fabric is easily wetted by water droplets. While water, cola, tea, coffee, milk, and orange juice droplets can stand on the surface of the coated fabric, showing an excellent superhydrophobicity. A mirror-like phenomenon is seen from the surface of the fabric when the PEI/TMSPA/SiO_2/DTMS fabric fixed on the glass was immersed in water (Fig. 5b), which is the formation of a solid–liquid–gas interface in air trapped by layered structures on the fabric surface and the surrounding environment to prevent water from penetrating into the superhydrophobic surface.[42] Meanwhile, the PEI/TMSPA/SiO_2/DTMS fabric showed superoleophilic properties, and oil droplets could be quickly absorbed and spread on the coated fabric surface (Fig. S4a†), since the oil surface tension (18.43 mN m^{-1}, in the case of *n*-hexane) is generally much less than that of water. Fig. 5c shows the photographs of 2 μL water droplets staying on the coated fabric surface and gradually evaporating. The droplet can remain spherical on the coated fabric for 5 minutes, indicating that the coated fabric possesses excellent superhydrophobic stability. Water droplet adhesion tests were carried out to investigate the adhesion behavior of the coated fabrics (Fig. 5d). The water droplet was observed to be elongated when moving away from the PEI/TMSPA/SiO_2/DTMS fabric, and then it was discharged from the coated fabric without any residue, indicating that coated fabric

 This journal is © The Royal Society of Chemistry 2022

Published on 22 December 2021. Downloaded on 1/19/2026 7:56:09 PM.

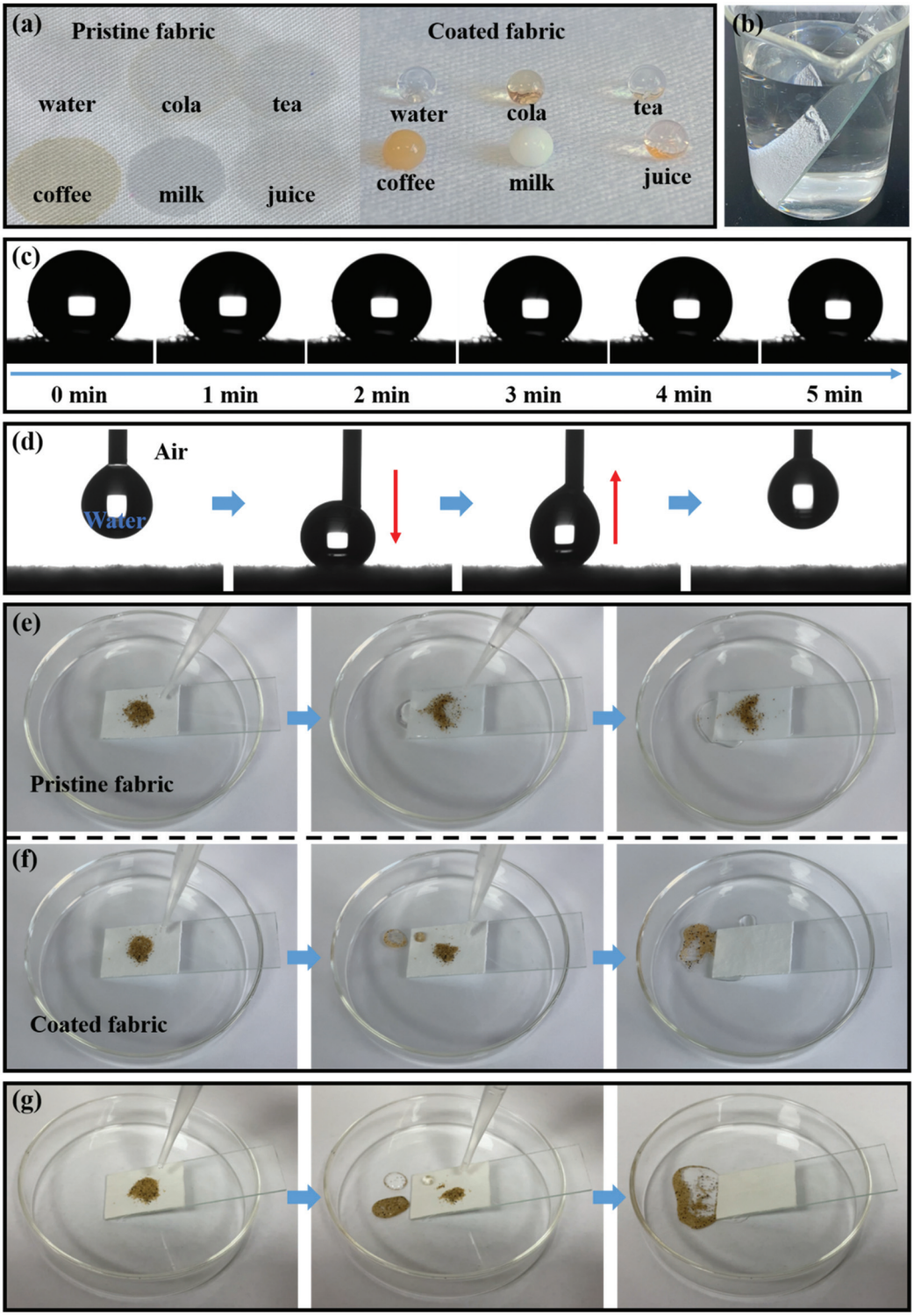

Fig. 5 (a) Photographs of aqueous droplets on original and coated fabrics. (b) The mirror appearance of the coated fabric that was forcibly put in water. (c) The water droplets staying on the coated fabric show stable superhydrophobicity. (d) Photos of the coated fabric, which repels a 4 μL water droplet. Optical images of self-cleaning tests of (e) pristine and (f) coated fabrics. (g) Self-cleaning performance test of the coated fabric which is contaminated by oil (*n*-hexane).

has excellent water repellences. Furthermore, the dynamic impinging behavior of water droplets on the PEI/TMSPA/SiO_2/DTMS fabrics was studied. When the droplet was dropped from a height of 5 cm above the surface of the fabric, the droplet first deforms into a flat cake shape, which does not penetrate the fabric, and then recovers into a sphere, similar

Published on 22 December 2021. Downloaded on 1/19/2026 7:56:09 PM.

to the pancake bounce[43] (Fig. S4b and c†). However, the water droplet never leaves the fabric surface, because part of the kinetic energy is transformed into viscous dissipation, and the other part is absorbed due to deformation of the substrate when water droplet impacts the soft substrate. The above results verify the good superhydrophobicity/superliphilicity of the PEI/TMSPA/SiO_2/DTMS fabric, ascribing to the solid–liquid–gas interface formation on the fabric surface and surface tension between water and oil.

In addition to cotton fabrics, a variety of substrates such as polyester, silk, ramie and acrylic fabrics, were used to fabricate superhydrophobic surfaces. The WCAs of all treated substrates are greater than 150°, and the photographs of water droplets staying on these substrates are displayed in Fig. S5.† Therefore, the preparation strategy discussed in this study shows significant versatility and flexibility for the fabrication of superhydrophobic fabrics.

Superhydrophobic fabric is inevitably contaminated by pollutants during use, which seriously affects the properties of superhydrophobic and oil/water separation materials. Thus, it is very important to combine self-cleaning properties with oil/water separation material to prolong its service life. Here, fine sand was used as a model contaminant in order to study the self-cleaning performance of PEI/TMSPA/SiO_2/DTMS fabrics. As shown in Fig. 5e, fine sand remained on the surface of the original fabric surface when water continuously dropped. While water droplets could roll off the coated fabric surface, taking away fine sand from the surface. Therefore, contaminations can be completed removed from the coated fabric surface by water (Fig. 5f). What is more, the self-cleaning properties of the coated fabrics can also be valid after contamination by oil (*n*-hexane), and water droplets can easily roll off the fabric surface without spreading (Fig. S4d†), indicating that the coated fabric can maintain its self-cleaning function even if it is contaminated by oil. Fig. 5g shows the self-cleaning test of the coated fabric, which was oil-contaminated. Apparently, water droplets could easily slide from the fabric surface by removing fine sand. The results are similar to the self-cleaning performance in the air. When in air, after being immersed in oil, oil pollutants penetrate, moisten, and adhere stably to the micro/nanostructure of the fabric, forming a lubricating liquid film, resulting in a smooth hydrophobic surface.[44] Therefore, dirt can be easily removed by passing the water through the oil to pollute the surface.

Stability of superhydrophobic PEI/TMSPA/SiO_2/DTMS fabrics

Usually, superhydrophobic materials are easy to lose superhydrophobic behavior if they are under harsh conditions, including high temperature, organic solvent, corrosive solution, and tape stripping. Here, the stability of the obtained PEI/TMSPA/SiO_2/DTMS fabric was thoroughly evaluated, including heat resistance, ultraviolet resistance, and chemical and mechanical stability. The thermal stability was evaluated by treatment of PEI/TMSPA/SiO_2/DTMS fabrics at different temperatures for 2 h. After treatment from 80 °C to 180 °C for 2 h, the WCA of the coated fabric showed no significant change, revealing that the superhydrophobic fabric possessed good thermal stability (Fig. 6a). Ultraviolet radiation from sunlight can seriously affect the coated fabric's long-term stability. Thus, we studied the influence of UV irradiation on the WCA of PEI/TMSPA/SiO_2/DTMS fabrics (Fig. 6b). It revealed that the WCA of the PEI/TMSPA/SiO_2/DTMS fabric was still above 150° after irradiation with a 1000 W strong UV source for 2 min each time 10 times, indicating that the coated fabric had good resistance to UV radiation. In addition, PEI/TMSPA/SiO_2/DTMS fabrics were placed in a variety of corrosive solutions to figure out their chemical stability. As shown in Fig. 6c, the WCA of the PEI/TMSPA/SiO_2/DTMS fabrics hardly changed after treatment in 1 M NaCl, HCl, and NaOH solutions for 12 h. At the same time, PEI/TMSPA/SiO_2/DTMS fabrics were treated in different organic solvents such as dichloromethane, *n*-hexane, ethyl acetate, DMF, ethylene glycol, toluene and acetone for 24 h to detect their chemical stability. All coated fabrics maintained the WCA above 150° after the treatment, showing good superhydrophobicity with organic solvent resistance (Fig. 6d).

Mechanical stability is crucial for real applications of superhydrophobic materials. Here, the mechanical stability of PEI/TMSPA/SiO_2/DTMS fabrics was qualitatively evaluated by the peeling test of adhesive tape. WCA was observed to remain above 150° after 60 cycles of peeling tests using adhesive tape (Fig. 6e). The treated PEI/TMSPA/SiO_2/DTMS fabric still maintained good water repellency, and the results revealed that SiO_2 and DTMS were successfully grafted on the PEI/TMSPA/SiO_2/DTMS fabric. In addition, washability is also important for fabrics. The washing test was carried out by stirring/washing coated fabrics in a detergent aqueous solution. Fig. 6f shows that the WCA of the coated fabric slightly decreased with the increase of washing cycles. After 8 cycles of washing, the surface almost maintained superhydrophobicity with the WCA of 149.9 ± 1.3°. These results showed that the superhydrophobic fabric has good mechanical stability, which can be attributed to the covalently cross-linked network formed between PEI and TMSPA-SiO_2.

Diverse application modes of superhydrophobic PEI/TMSPA/SiO_2/DTMS fabrics

Superhydrophobic cotton fabrics show great potential in oil/water separation application because of their porosity and special wettability (superhydrophobic/superoleophilic properties). The obtained coated fabric can be employed as an oil separation material for the oil/water mixture. The typical gravity-driven separation process using PEI/TMSPA/SiO_2/DTMS fabrics is displayed in Fig. 7a and Movie S1.† The PEI/TMSPA/SiO_2/DTMS fabric was fixed between the separation devices and the mixture of methyl blue-dyed water and Sudan IV dyed dichloromethane was poured into the upper tube of the separation device. It was observed that the red-dyed dichloromethane was rapidly passed through the coated fabric because of gravity and could be collected, while the blue water layer was excluded throughout the process and remained at the top. In addition, the separation efficiency, flux and recyclability

 This journal is © The Royal Society of Chemistry 2022

Published on 22 December 2021. Downloaded on 1/19/2026 7:56:09 PM.

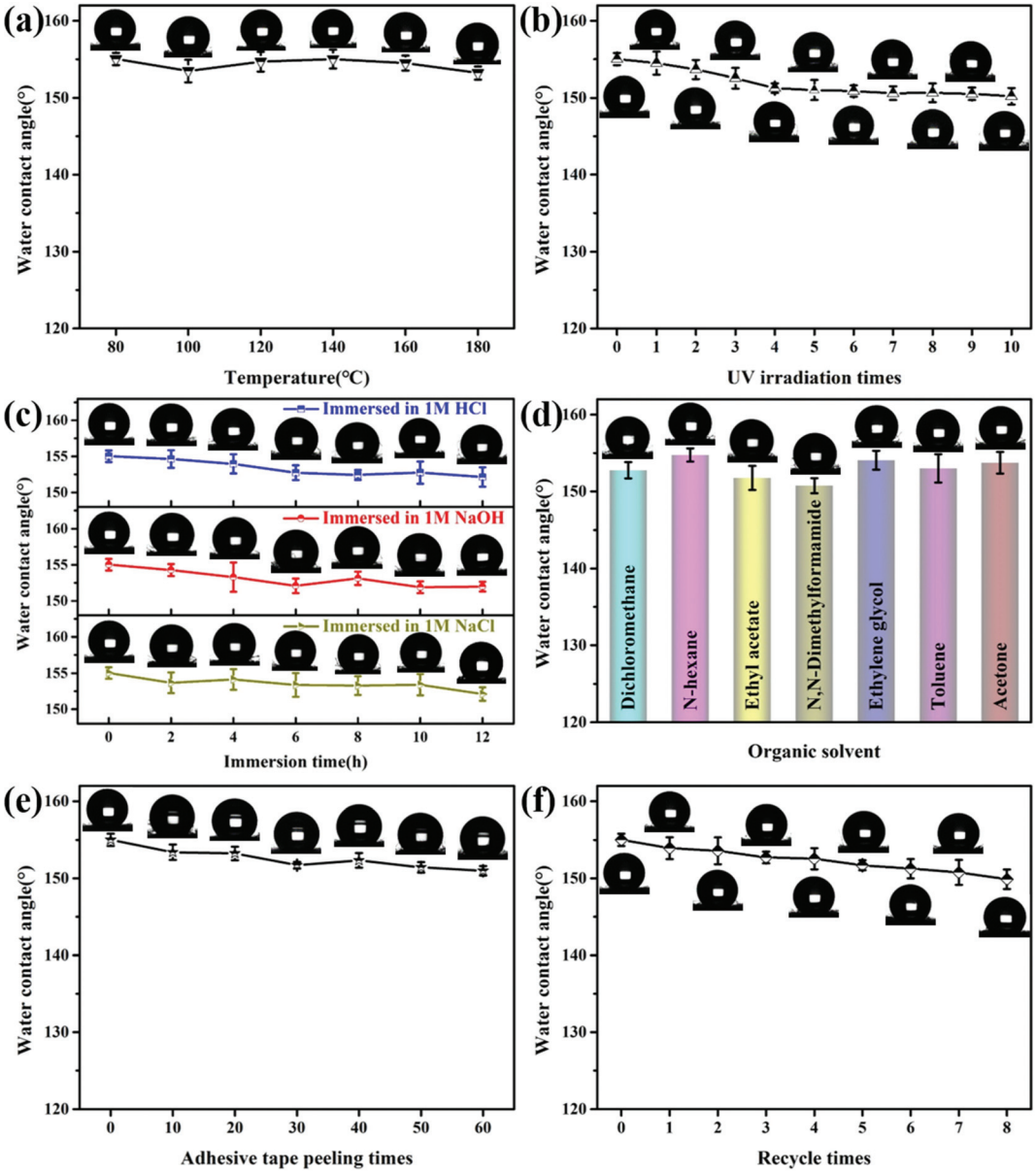

Fig. 6 Variations in the WCA of the PEI/TMSPA/SiO_2/DTMS fabric after (a) heating at different temperatures for 2 h, (b) UV irradiation with different times, (c) treatment in 1 M NaCl, HCl, and NaOH solutions for different times, (d) immersion in different organic solvents for 24 h, (e) adhesive tape peeling test and (f) washing test.

were tested and calculated to assess the separation property of PEI/TMSPA/SiO_2/DTMS fabrics. The superhydrophobic fabric has a significant separation capacity for a variety of insoluble oil/water mixtures. Their separation efficiency could reach above 99.68% (Fig. 7c). The permeation fluxes of dichloromethane, *n*-hexane, petroleum ether, toluene, and chloroform were 10016.49 ± 78.37, 2098.10 ± 40.40, 2579.01 ± 59.61, 2397.85 ± 63.20, and 8675.88 ± 84.51 L m^{-2} h^{-1}, respectively. The difference in the separation flux can be attributed to the different viscosity of oils.[45] More importantly, for the dichloromethane/water mixture, the separation efficiency of the PEI/TMSPA/SiO_2/DTMS fabric was still higher than 98.20% after 18 repeated separation cycles (Fig. 7d), indicating that the coated fabric has stable separation performance and excellent reusability.

Fig. 7b shows a hypothetical schematic of the coated fabric separating oil/water mixtures to understand the separation mechanism. Due to the excellent superhydrophobicity of the PEI/TMSPA/SiO_2/DTMS fabric, water droplets are easily excluded from the coated fabric surface. When oil contacts the coated fabric, the fabric surface was immediately wetted and penetrated by oil because of its superoleophilicity and hierarchical porous structure. Thus, the oil layer on the fabric surface allows water to unfold on the surface with a lower WCA, while oil can easily penetrate the fabric, resulting in successfully obtaining the separation of the oil/water mixture.

Published on 22 December 2021. Downloaded on 1/19/2026 7:56:09 PM.

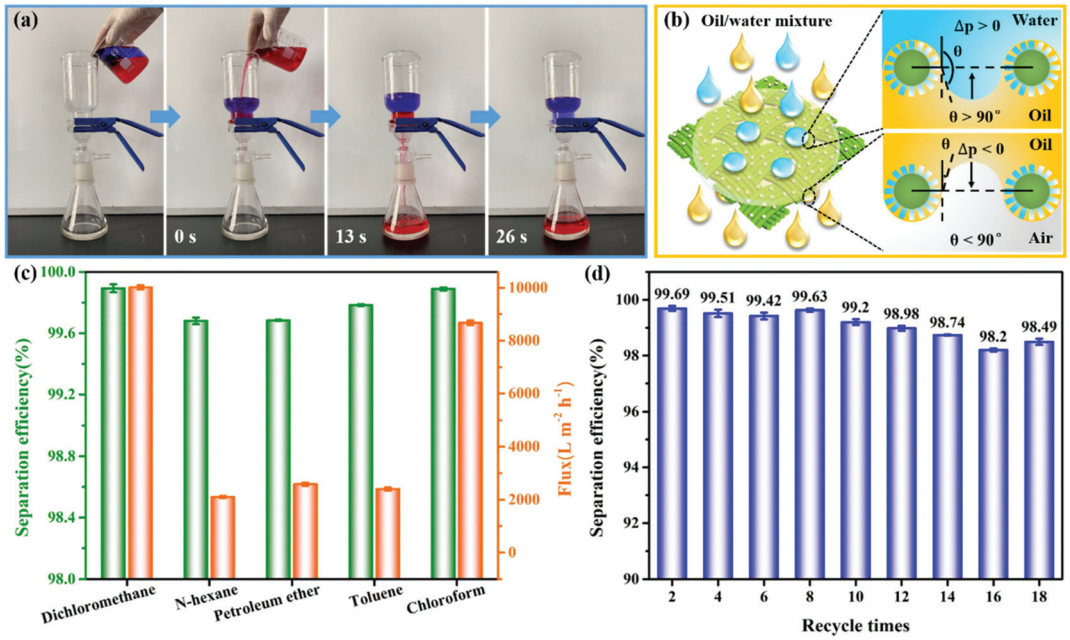

Fig. 7 (a) Schematic of oil/water separation using PEI/TMSPA/SiO_2/DTMS fabrics. (b) Schematic of oil/water mixture separation mechanism of coated fabrics. (c) Separation efficiencies and fluxes of different oil/water mixtures. (d) The separation efficiency of the dichloromethane/water mixture after multiple separation cycles.

Models of oil/water wetting are used to learn the separation process (Fig. 7b, right).[45] According to Laplace equation, the critical-resistant pressure is determined by eqn (5):

$$\Delta p = \frac{2\gamma}{R} = -\frac{l\gamma\cos\theta_a}{A} \quad (5)$$

where γ represents interfacial tension, R represents pore radius, l represents the perimeter of the hole, A represents the hole cross-sectional area, and θ_a represents the contact angle. PEI/TMSPA/SiO_2/DTMS fabric has WCA of 155.0 ± 0.8° and OCA of ~0°. According to eqn (5), we can know $\Delta p > 0$ of water while $\Delta p < 0$ of oil. The result indicates that before being fully wetted with water, the coated fabric surface requires bearing some external pressure, and oil can easily pass through the coated fabric without external pressure. Thus, for the oil/water mixture separation, the oil can rapidly pass through the coated fabric, while water is retained on the top of the fabric, successfully separating the water and oil.

Superhydrophobic fabrics are limited by the separation of substantial stratified oil/water mixtures, so it is a challenge to develop novel application patterns to enlarge the application range of superhydrophobic fabrics. The PEI/TMSPA/SiO_2/DTMS fabric can be used in adsorbent materials to remove oil from water due to both superhydrophobicity and superoleophilicity. Fig. S6† shows the selective adsorption of coated fabrics on *n*-hexane (Fig. S6a–c†) and chloroform (Fig. S6d–f†) in water. However, for oil spill cleanup, the adsorption capacity of superhydrophobic fabric is limited. Superhydrophobic porous materials such as metal mesh can usually float on the water surface and collect oil droplets on the water surface without manual operation. We speculate that a boat made of superhydrophobic fabrics can float on the water surface to collect oil spills, and the flow chart is shown in Fig. 8a. Fig. 8b shows that the superhydrophobic fabric could be made into a mini boat. The superhydrophobic mini boat could easily float on the water surface (Fig. 8c), and there is an air cushion on the bottom of the boat (Fig. 8d). The superhydrophobic mini boat could carry several metal screws (5.9784 g) and float on the water surface (Fig. 8e and f and Movie S2†). The load-bearing capacity of the mini boat on the water is about eight times that of its own weight (0.7347 g).

Fig. 8g and Movie S3† demonstrate the self-driven oil spill cleanup process. First, some oil droplets (Sudan IV dyed octane) were added to the water surface. Then, the superhydrophobic mini boat was put on the water surface with octane. When the fabric contacted with oil, it first absorbed oil until the fabric was saturated and the excess oil could penetrate into the boat and automatically gather in the boat further. In this process, water was excluded and cannot pass through the boat wall. Finally, the collected oil can be pumped out of the mini boat for recovery. To study the reusability of the superhydrophobic mini boat, the mass change of the boat before and after oil collection was recorded, and its separation efficiency was calculated. The cleanup efficiency of the boat for octane can still reach 95.09% after 9 cycles, indicating its good reusability (Fig. 8h).

Interestingly, the good load-bearing capacity of superhydrophobic mini boat can be used to study the buoyancy of superhydrophobic cotton fabric. We find that the maximum deadweight of the boat is 6.7131 g if the weight of the boat is

 This journal is © The Royal Society of Chemistry 2022

Published on 22 December 2021. Downloaded on 1/19/2026 7:56:09 PM.

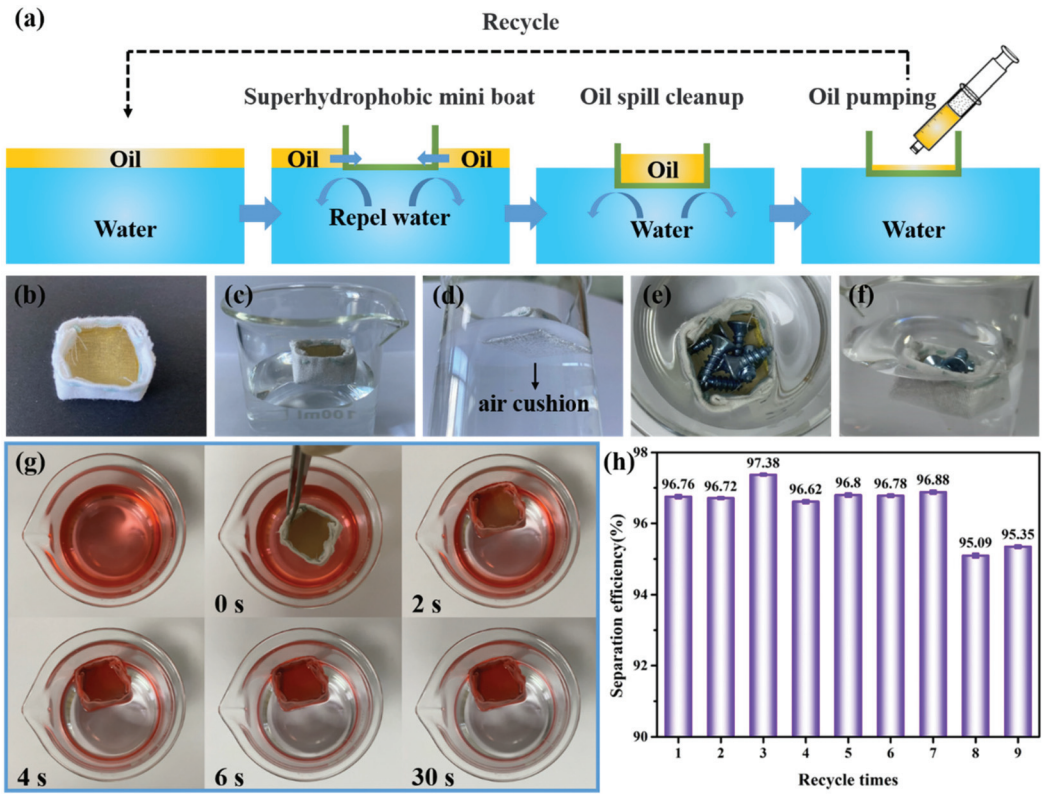

Fig. 8 (a) Schematic of oil spill cleaning of the superhydrophobic mini boat. (b) Optical image of the superhydrophobic mini boat. (c) Front view and (d) upward view of a superhydrophobic mini boat floating on the water surface. (e) downward view and (f) front view of the superhydrophobic mini boat with several screws floating on the water surface. (g) Self-driven oil spill cleanup process of the superhydrophobic mini boat. (h) Oil spill cleanup efficiency of the superhydrophobic mini boat under multiple cycles.

included. However, the volume of the boat is 4.32 cm^3. According to the Archimedean principle, the carrying capacity of the boat on the water surface should be 4.32 g. This suggests that in addition to the 4.32 g buoyancy associated with the boat volume, there is an additional buoyancy to support the 2.3931 g extra load. One of the contributions to additional buoyancy comes from the plastron effect,[46] where the air film trapped around the outer surface of the fabric provides additional water displacement and thus provides additional buoyancy. It can be seen from Fig. 8e and f that even though the upper edge of the boat is leveled with water and even partially below the water surface, the boat can still float, which is ascribed to the extremely low surface energy of superhydrophobic fabrics. Thus, surface tension associated with the upper perimeter of the boat is another contribution to extra buoyancy.

Surprisingly, the prepared PEI/TMSPA/SiO_2/DTMS fabric was also able to effectively separate oil from the oil-in-water emulsion. The coated fabric was placed in a toluene-in-water emulsion and allowed to stand. After oil droplets were mostly absorbed on the coated fabric, the emulsion gradually became transparent. Photographs and optical microscope images before and after the emulsion separation by the superhydrophobic fabric are shown in Fig. S7.† The optical microscope image of a pristine emulsion showed a large number of oil droplets, while no droplets were found in the separated liquid, confirming the complete oil-in-water emulsion separation. In addition, as shown in Fig. S7,† the size of oil droplets in the pristine emulsion was distributed between 2 and 10 μm with an average size of 5.29 μm, while the filtrate was clear and no droplets were detected. In order to further evaluate the emulsion separation ability, toluene content in the separated water was determined, and the emulsion separation efficiency reached 96.12% by calculation.

4. Conclusion

In summary, we developed a facile yet effective strategy to manufacture eco-friendly and durable superhydrophobic fabrics, which achieved efficient oil/water separation and oil spill cleanup. The hydrolysis and condensation of TMSPA and DTMS were co-modified on the surface of silica, and the 1,4-conjugate addition reaction between the acrylic group of TMSPA and the primary amine group of PEI formed a covalently cross-linked rough network structure. The covalently cross-linked network could fix the hierarchical rough structure and reduce surface energy because of abundant hydrophobic alkyl chains of DTMS, so the obtained cotton fabric has excellent superhydrophobicity. The obtained superhydrophobic

Published on 22 December 2021. Downloaded on 1/19/2026 7:56:09 PM.

fabric showed excellent thermal stability, chemical stability and good mechanical stability. By virtue of superhydrophobicity, superoleophilicity and inherent porous structure, the modified fabric achieved high separation efficiency of a variety of oil/water mixtures and oil-in-water emulsions with surfactant stabilization. In addition, the fabricated superhydrophobic mini boat further showed good oil spill cleanup efficiency and cycle times. Therefore, the unique advantages including mildness, environmental friendliness and one-step manufacturing process of the PEI/TMSPA/SiO_2/DTMS fabric make it have broad prospects in diversified applications in actual oil/water separation and oil spill cleanup in the near future.

Conflicts of interest

The authors declare no competing financial interest.

Acknowledgements

This work was supported by the National Natural Science Foundation of China (No. 21774098) and the Opening Project of State Key Laboratory of Polymer Materials Engineering (Sichuan University) (Grant No. sklpme2019-4-26).

References

1 R. K. Gupta, G. J. Dunderdale, M. W. England and A. Hozumi, Oil/water separation techniques: a review of recent progresses and future directions, *J. Mater. Chem. A*, 2017, **5**, 16025–16058.

2 R. Zhu, M. Liu, Y. Hou, L. Zhang, M. Li, D. Wang, D. Wang and S. Fu, Biomimetic Fabrication of Janus Fabric with Asymmetric Wettability for Water Purification and Hydrophobic/Hydrophilic Patterned Surfaces for Fog Harvesting, *ACS Appl. Mater. Interfaces*, 2020, **12**, 50113–50125.

3 M. Padaki, R. Surya Murali, M. S. Abdullah, N. Misdan, A. Moslehyani, M. A. Kassim, N. Hilal and A. F. Ismail, Membrane technology enhancement in oil–water separation. A review, *Desalination*, 2015, **357**, 197–207.

4 H. Li, P. Mu, J. Li and Q. Wang, Inverse desert beetle-like ZIF-8/PAN composite nanofibrous membrane for highly efficient separation of oil-in-water emulsions, *J. Mater. Chem. A*, 2021, **9**, 4167–4175.

5 A. Li, Q. Rao, F. Liang, L. Song, X. Zhan, F. Chen, J. Chen and Q. Zhang, Polyhydroxy Group Functionalized Zwitterion for a Polyamide Nanofiltration Membrane with High Water Permeation and Antifouling Performance, *ACS Appl. Polym. Mater.*, 2020, **2**, 3850–3858.

6 C. Teas, S. Kalligeros, F. Zanikos, S. Stournas, E. Lois and G. Anastopoulos, Investigation of the effectiveness of absorbent materials in oil spills clean up, *Desalination*, 2001, **140**, 259–264.

7 N. Wang, D. Xiong, Y. Deng, Y. Shi and K. Wang, Mechanically Robust Superhydrophobic Steel Surface with Anti-Icing, UV-Durability, and Corrosion Resistance Properties, *ACS Appl. Mater. Interfaces*, 2015, **7**, 6260–6272.

8 T. Zhu, Y. Cheng, J. Huang, J. Xiong, M. Ge, J. Mao, Z. Liu, X. Dong, Z. Chen and Y. Lai, A transparent superhydrophobic coating with mechanochemical robustness for anti-icing, photocatalysis and self-cleaning, *Chem. Eng. J.*, 2020, **399**, 125746.

9 G. Luo, L. Wen, K. Yang, X. Li, S. Xu, P. Pi and X. Wen, Robust and durable fluorinated 8-MAPOSS-based superamphiphobic fabrics with buoyancy boost and drag reduction, *Chem. Eng. J.*, 2020, **383**, 123125.

10 M. Yu, M. Liu and S. Fu, Slippery Antifouling Polysiloxane-Polyurea Surfaces with Matrix Self-Healing and Lubricant Self-Replenishing, *ACS Appl. Mater. Interfaces*, 2021, **13**, 32149–32160.

11 H. Wang, X. Zhang, Z. Liu, Y. Zhu, S. Wu and Y. Zhu, A superrobust superhydrophobic PSU composite coating with self-cleaning properties, wear resistance and corrosion resistance, *RSC Adv.*, 2016, **6**, 10930–10937.

12 J. Zhang, L. Zhang and X. Gong, Large-Scale Spraying Fabrication of Robust Fluorine-Free Superhydrophobic Coatings Based on Dual-Sized Silica Particles for Effective Antipollution and Strong Buoyancy, *Langmuir*, 2021, **37**, 6042–6051.

13 Y. Lai, F. Pan, C. Xu, H. Fuchs and L. Chi, In Situ Surface-Modification-Induced Superhydrophobic Patterns with Reversible Wettability and Adhesion, *Adv. Mater.*, 2013, **25**, 1682–1686.

14 H. Zhao, D. Benetti, X. Tong, H. Zhang, Y. Zhou, G. Liu, D. Ma, S. Sun, Z. M. Wang, Y. Wang and F. Rosei, Efficient and stable tandem luminescent solar concentrators based on carbon dots and perovskite quantum dots, *Nano Energy*, 2018, **50**, 756–765.

15 T. Yu, F. Halouane, D. Mathias, A. Barras, Z. Wang, A. Lv, S. Lu, W. Xu, D. Meziane, N. Tiercelin, S. Szunerits and R. Boukherroub, Preparation of magnetic, superhydrophobic/superoleophilic polyurethane sponge: Separation of oil/water mixture and demulsification, *Chem. Eng. J.*, 2020, **384**, 123339.

16 L. Zhong, H. Tao and X. Gong, Superhydrophobic Poly(l-lactic acid) Membranes with Fish-Scale Hierarchical Microstructures and Their Potential Application in Oil–Water Separation, *Langmuir*, 2021, **37**, 6765–6775.

17 J. Zhang, L. Zhang and X. Gong, Design and fabrication of polydopamine based superhydrophobic fabrics for efficient oil–water separation, *Soft Matter*, 2021, **17**, 6542–6551.

18 M. Wu, G. Shi, W. Liu, Y. Long, P. Mu and J. Li, A Universal Strategy for the Preparation of Dual Superlyophobic Surfaces in Oil–Water Systems, *ACS Appl. Mater. Interfaces*, 2021, **13**, 14759–14767.

19 F. Guan, Z. Song, F. Xin, H. Wang, D. Yu, G. Li and W. Liu, Preparation of hydrophobic transparent paper via using polydimethylsiloxane as transparent agent, *J. Bioresour. Bioprod.*, 2020, **5**, 37–43.

 This journal is © The Royal Society of Chemistry 2022

Published on 22 December 2021. Downloaded on 1/19/2026 7:56:09 PM.

20 D. W. Wei, H. Wei, A. C. Gauthier, J. Song, Y. Jin and H. Xiao, Superhydrophobic modification of cellulose and cotton textiles: Methodologies and applications, *J. Bioresour. Bioprod.*, 2020, **5**, 1–15.
21 J. Lin, C. Zheng, W. Ye, H. Wang, D. Feng, Q. Li and B. Huan, A facile dip-coating approach to prepare SiO_2/fluoropolymer coating for superhydrophobic and superoleophobic fabrics with self-cleaning property, *J. Appl. Polym. Sci.*, 2015, **132**, 41458.
22 J. Wang, F. Han, B. Liang and G. Geng, Hydrothermal fabrication of robustly superhydrophobic cotton fibers for efficient separation of oil/water mixtures and oil-in-water emulsions, *J. Ind. Eng. Chem.*, 2017, **54**, 174–183.
23 X. Xiao, G. Cao, F. Chen, Y. Tang, X. Liu and W. Xu, Durable superhydrophobic wool fabrics coating with nanoscale Al_2O_3 layer by atomic layer deposition, *Appl. Surf. Sci.*, 2015, **349**, 876–879.
24 Y. Cheng, T. Zhu, S. Li, J. Huang, J. Mao, H. Yang, S. Gao, Z. Chen and Y. Lai, A novel strategy for fabricating robust superhydrophobic fabrics by environmentally-friendly enzyme etching, *Chem. Eng. J.*, 2019, **355**, 290–298.
25 D. Caschera, A. Mezzi, L. Cerri, T. de Caro, C. Riccucci, G. M. Ingo, G. Padeletti, M. Biasiucci, G. Gigli and B. Cortese, Effects of plasma treatments for improving extreme wettability behavior of cotton fabrics, *Cellulose*, 2014, **21**, 741–756.
26 Z. Chen, Z. Lv, Y. Sun, Z. Chi and G. Qing, Recent advancements in polyethyleneimine-based materials and their biomedical, biotechnology, and biomaterial applications, *J. Mater. Chem. B*, 2020, **8**, 2951–2973.
27 A. Das, J. Deka, K. Raidongia and U. Manna, Robust and Self-Healable Bulk-Superhydrophobic Polymeric Coating, *Chem. Mater.*, 2017, **29**, 8720–8728.
28 D. Parbat, S. Gaffar, A. M. Rather, A. Gupta and U. Manna, A general and facile chemical avenue for the controlled and extreme regulation of water wettability in air and oil wettability under water, *Chem. Sci.*, 2017, **8**, 6542–6554.
29 D. Parbat and U. Manna, Synthesis of 'reactive' and covalent polymeric multilayer coatings with durable superoleophobic and superoleophilic properties under water, *Chem. Sci.*, 2017, **8**, 6092–6102.
30 A. M. Rather, A. Shome, S. Kumar, B. K. Bhunia, B. B. Mandal, H. K. Srivastava and U. Manna, Alkali metal-ion assisted Michael addition reaction in controlled tailoring of topography in a superhydrophobic polymeric monolith, *J. Mater. Chem. A*, 2018, **6**, 17019–17031.
31 M. Sohail, B. Ashfaq, I. Azeem, A. Faisal, S. Y. Doğan, J. Wang, H. Duran and B. Yameen, A facile and versatile route to functional poly(propylene) surfaces via UV-curable coatings, *React. Funct. Polym.*, 2019, **144**, 104366.
32 M. E. Yazdanshenas and M. Shateri-Khalilabad, One-Step Synthesis of Superhydrophobic Coating on Cotton Fabric by Ultrasound Irradiation, *Ind. Eng. Chem. Res.*, 2013, **52**, 12846–12854.
33 Q. Shang, C. Liu, J. Chen, X. Yang, Y. Hu, L. Hu, Y. Zhou and X. Ren, Sustainable and Robust Superhydrophobic Cotton Fabrics Coated with Castor Oil-Based Nanocomposites for Effective Oil–Water Separation, *ACS Sustainable Chem. Eng.*, 2020, **8**, 7423–7435.
34 X. Han and X. Gong, In Situ, One-Pot Method to Prepare Robust Superamphiphobic Cotton Fabrics for High Buoyancy and Good Antifouling, *ACS Appl. Mater. Interfaces*, 2021, **13**, 31298–31309.
35 P. Rekha, V. Sharma and P. Mohanty, Synthesis of cyclophosphazene bridged mesoporous organosilicas for CO_2 capture and Cr(VI) removal, *Microporous Mesoporous Mater.*, 2016, **219**, 93–102.
36 X. Dong, S. Gao, J. Huang, S. Li, T. Zhu, Y. Cheng, Y. Zhao, Z. Chen and Y. Lai, A self-roughened and biodegradable superhydrophobic coating with UV shielding, solar-induced self-healing and versatile oil–water separation ability, *J. Mater. Chem. A*, 2019, **7**, 2122–2128.
37 C. Zhang, Y. Ou, W.-X. Lei, L.-S. Wan, J. Ji and Z.-K. Xu, $CuSO_4/H_2O_2$-Induced Rapid Deposition of Polydopamine Coatings with High Uniformity and Enhanced Stability, *Angew. Chem., Int. Ed.*, 2016, **55**, 3054–3057.
38 J. Li, W. Tang, H. Yang, Z. Dong, J. Huang, S. Li, J. Wang, J. Jin and J. Ma, Enhanced-electrocatalytic activity of $Ni_{1-x}Fe_x$ alloy supported on polyethyleneimine functionalized MoS_2 nanosheets for hydrazine oxidation, *RSC Adv.*, 2014, **4**, 1988–1995.
39 A. A. Qaiser, M. M. Hyland and D. A. Patterson, Surface and Charge Transport Characterization of Polyaniline-Cellulose Acetate Composite Membranes, *J. Phys. Chem. B*, 2011, **115**, 1652–1661.
40 J. H. Drese, S. Choi, R. P. Lively, W. J. Koros, D. J. Fauth, M. L. Gray and C. W. Jones, Synthesis–Structure–Property Relationships for Hyperbranched Aminosilica CO_2 Adsorbents, *Adv. Funct. Mater.*, 2009, **19**, 3821–3832.
41 Y. Liu, K. Ai and L. Lu, Polydopamine and Its Derivative Materials: Synthesis and Promising Applications in Energy, Environmental, and Biomedical Fields, *Chem. Rev.*, 2014, **114**, 5057–5115.
42 L. Wen, Y. Tian and L. Jiang, Bioinspired Super-Wettability from Fundamental Research to Practical Applications, *Angew. Chem., Int. Ed.*, 2015, **54**, 3387–3399.
43 Y. Liu, L. Moevius, X. Xu, T. Qian, J. M. Yeomans and Z. Wang, Pancake bouncing on superhydrophobic surfaces, *Nat. Phys.*, 2014, **10**, 515–519.
44 T.-S. Wong, S. H. Kang, S. K. Y. Tang, E. J. Smythe, B. D. Hatton, A. Grinthal and J. Aizenberg, Bioinspired self-repairing slippery surfaces with pressure-stable omniphobicity, *Nature*, 2011, **477**, 443–447.
45 W. Ma, Y. Ding, Y. Li, S. Gao, Z. Jiang, J. Cui, C. Huang and G. Fu, Durable, self-healing superhydrophobic nanofibrous membrane with self-cleaning ability for highly-efficient oily wastewater purification, *J. Membr. Sci.*, 2021, **634**, 119402.
46 Q. Pan and M. Wang, Miniature Boats with Striking Loading Capacity Fabricated from Superhydrophobic Copper Meshes, *ACS Appl. Mater. Interfaces*, 2009, **1**, 420–423.